

DOI: <http://doi.org/10.52716/jprs.v12i1.599>

An Experimental Study of the Effect of Different Blending Ratios of Dual and Triple Fuel Mixtures (Gasoline-Hydrogen-Ethanol) on Laminar Flame Speed

Oras Khudhayer Obayes^{1*}, Haroun A. K. Shahad²¹Power Mechanics Department, Al-Furat Al-Awsat Technical University (ATU), Technical Institute of Babylon²Department of Mechanical Engineering, University of Babylon*Corresponding Author E-mail: oras.obais@atu.edu.iq6th Iraq Oil and Gas Conference, 29-30/11/2021This work is licensed under a [Creative Commons Attribution 4.0 International License](https://creativecommons.org/licenses/by/4.0/).

Abstract

In a centrally ignited constant volume chamber, an experimental research on the laminar flame speed of premixed gasoline/ethanol/hydrogen/air mixtures is undertaken at varied initial pressures (0.1-0.3 MPa), constant initial temperature (593 K), and variable equivalency ratios (0.75-1.5). The mixing method is based on the energy replacement principle, and various component blending ratios are tested. This has necessitated the construction of a specific laboratory experimental equipment. The flame speeds are measured using the Shelerian photography technique using a high-speed camera. The results reveal that adding hydrogen to dual fuel mixtures has a considerable impact on stretched laminar flame speed. The stretched laminar flame speeds for 20 percent H₂-80 percent G, 40 percent H₂-60 percent G, and 60 percent H₂-40 percent G are 3.71 m/s, 7.329 m/s, and 11.0267 m/s, respectively, at 0.1 MPa initial pressure and stoichiometric mixture. For 20 percent H₂-80 percent G, 40 percent H₂-60 percent G, and 60 percent H₂-40 percent G mixtures, the un-stretched flame speed at atmospheric pressure and stoichiometric is computed and found to be 1.23 m/s, 3.67 m/s, and 7.093 m/s, respectively. When the initial pressure is increased, both stretched and un-stretched flame rates drop.

The results of the triple fuel mixes demonstrate that the influence of ethanol addition on the stretched laminar flame speed is significant at constant hydrogen blending ratios, with 2.24 m/s at 20% H₂-16% E-64 percent G and 2.68 m/s at 20% H₂-32 % E-48 % G at 0.1 MPa for stoichiometric mixture. For dual fuel combinations, the effect of starting pressure on stretched and un-stretched flame speeds is the same. Where the flame speed has a maximum value for stoichiometric combustion, the equivalence ratio has a greater effect on flame speed.

Keywords: Laminar Flame Speed, Flame Stretch Rate, Fuel blending, Liquid Fuel, dual Fuel Mixture, Triple Fuel Mixture

1. Introduction

Visible chemical component experiencing extremely exothermic chemical reaction takes place in a narrow zone with the evolution of heat," according to the most applicable definition of flames. In a combustion reaction, the flame speed is the observed rate of expansion of the flame front [1]. The speed at which a flame burns is an important aspect of the combustion properties of a fuel. It has an impact on the design and performance of combustion systems. Stretched laminar flame speed encapsulates the fundamental information about a specific mixture's diffusivity, un-reactivity, and exothermicity, and is thus widely used to characterize flames. The detection of flame front arrival along a specific space necessitates a special approach for measuring flame speed, therefore many investigators worked hard to discover the various techniques for measuring flame speed. The stagnation flow arrangement was used by [2] to assess the laminar flame speed of an ethane/air combination diluted with helium or nitrogen before the flame transitioned from planar to Bunsen flame. GRI-Mach 3.0 numerical simulation was used to compare the results. The laminar flame speed of ethane/air/helium was higher than expected, but the ethane/air/nitrogen dilution was more accurate. To vaporize liquid fuels of n-heptane/air and n-decane/air mixtures, a preheating process was utilized [3]. At 500 degrees Celsius, measurements were made on a gasoline surrogate fuel made up of a blend of n-heptane and iso-octane. The surrogate fuel's laminar flame speed was compared to that of actual gasoline and the principal reference fuel (PRF) model. [4] expanded the adiabatic flat flame method to measure the laminar flame speed of ethane, propane, n-butane, and isobutene. At 500 K and atmospheric pressure, [5] evaluated laminar flame speeds of n-decane/air mixtures with and without dilution. The reported flame speeds differed significantly from those predicted by published kinetic models, including one that was confirmed using high temperature data from flow reactor, jet stirred reactor, shock tube ignition delay, and burner stabilized flame tests. [6] examined the flame speed of an H₂-CO-CO₂ combination over a range of beginning temperatures and compared the stretched flame to simulated results using GRI Mach 3.0 [7] and the H₂-CO mechanism of [8]. At 700 K, the strained laminar flame speeds for a lean mixture of 50: 50 H₂-CO were

measured. The goal has been to develop a complete, kinetically accurate model that can forecast a wide range of H₂- CO combustion data.

According to [9], a higher engine compression ratio enhances engine efficiency by increasing flame speed. The key physico-chemical information in evaluating the flame propagation process and turbulent flame research is laminar flame characteristic, namely laminar flame speed. In addition, chemical kinetics models are frequently validated using laminar flame speed [10]. The ratio of fuel to air has a considerable impact on flame speed. With a little richer mixture, the maximum flame velocities can be achieved. The flame speed reduces as the mixture becomes leaner or richer. In the case of lean mixes, less thermal energy is generated, resulting in a lower flame temperature. Incomplete combustion occurs in very rich mixtures, resulting in the release of less thermal energy [11]. [12] Reported on the experimental determination of laminar flame speed for iso-octane mixtures of butanol and ethanol. Using the spherical expanding flame approach in a constant volume vessel, new data sets of laminar flame speed are provided. There is also a volume. The first results for pure fuels (iso-octane, ethanol, and butanol) at a starting pressure of 0.1 MPa and a temperature of 400 K, with equivalency ratios ranging from 0.8 to 1.4, were given in this study. There are also new statistics on laminar flame speed for three fuel blends comprising up to 75% alcohol by liquid content. A correlation is proposed based on these new experimental results to determine the laminar flame speed of any butanol or ethanol blend iso-octane–air mixture. [13] provided experimental data on the effect of the fuel/air ratio on the combustion characteristics of a direct injection spark ignition engine fueled with a syngas of equal molar ratio H₂-CO composition. At lower speeds, the effect of the fuel-to-air ratio was more obvious in the early stages of combustion. In a centrally ignited constant volume chamber, [14] investigated laminar flame speed of premixed Iraqi LPG-hydrogen-air flames at varying initial pressures (0.1-0.3 MPa) and initial temperatures of (308 K). Furthermore, the analyzed hydrogen blends ranged from 0-80% by volume, while the tested equivalency ratios of air/fuel mixture ranged from (0.8 - 1.3). The stretched laminar flame speed of the LPG-air mixture is reduced from (2.2-1.5 m/s) when the initial pressure is increased from 1 bar to 3 bar. [15] published a review study on the flame speed and burning velocity of gaseous and liquid fuels, two

significant components of fuel combustion characteristics. Both have an impact on the design and performance of combustion systems.

The goal of this research is to determine the stretched laminar flame speed of the triple fuel mixtures of gasoline, hydrogen, and ethanol, as well as to compute the unstretched flame speed. At a constant initial temperature, the effects of initial pressure, equivalence ratio, and blending ratio will be examined.

2. Experimental Rig Setup

The flame speeds are measured using the constant volume combustion chamber method and the Schlieren photography technique. Fuel supply unit, Fuel Injection unit, Constant volume combustion chamber unit, Hot Air Tank unit, Ignition System Unit, Fuel Injection and Control Unit, Capturing unit, and Measuring Instruments make up the entire rig configuration, as shown in Figure (1).

A. Fuel Supply Unit

Fuel is supplied by a pressurized air at a pressure of about 2 bars. This unit consists of air compressor, pressure regulator, Borden gauge, air pressure distributor and small gasoline fuel tank, small ethanol fuel tank and hydrogen bottle as shown in Figure (2).

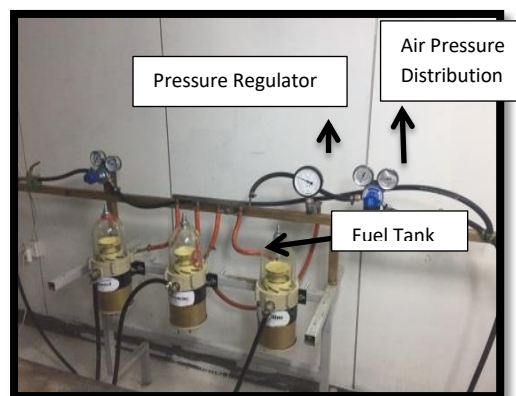
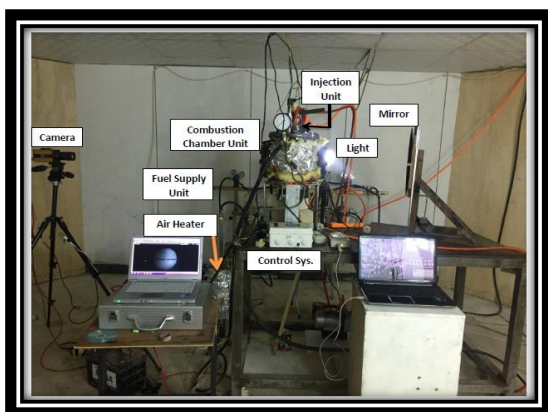


Fig. (1): Photograph of the Experimental Apparatus Fig. (2) Fuel Supply Unit

B. Fuel Injection Unit

This unit consists of two liquid fuel injectors and a small pre-chamber. Two electronic fuel injectors (one for gasoline and the other for ethanol) with a certain pulse width (PW) are used to inject the required (pre-calculated) amount of each fuel. The injectors are mounted on the pre-chamber attached to the main chamber in order to protect them

from high temperature of the combustion chamber. The pre-chamber is a small cylinder with a capacity of 24 ml which is equivalent to 0.3 % of combustion chamber volume. The amount of each fuel to be injected depends on the required mixture equivalence ratio and fuels blending ratio. A special control unit is designed to control the injection of each fuel in the pre-chamber which is then vaporized by hot air before entering the main chamber.

C. Constant Volume Combustion Chamber

It's a (190 mm) inner diameter, (250 mm) height, and (10 mm) wall thickness iron cylinder with a volume of (7.2 L). It is composed of iron and has two (20 mm) thick upper and lower flanges with a diameter of (300 mm) to withstand the tremendous pressure and temperature generated by combustion. The cylinder has electrodes in the center that are connected to the ignition system. The pressure of combustion is measured using a pressure gauge. A safety valve is installed in the chamber. To scavenge the chamber, a vacuum pump is employed. Photographs can be taken through two glass windows on opposing ends of the space.

D. Air Heating Unit

The used air must be heated to a temperature higher than the condensation temperature of the vapor of both liquid fuels. The hot air is supplied from the hot air tank which is cylindrical air (outer diameter = 45 cm, length =37 cm, and thickness =6 mm) which is made of stainless steel. The tank is heated by an electric heater type (COOPERHEAT), type VTP 230 -240 V, power of 30 W/m, with 15 m length. In order to keep the air temperature constant, the combustion chamber is heated by electric heater type ART.NO.ES.1520 with 220 V- 240 V, 50-60 HZ, 1500 W to a temperature that prevents fuel vapor condensation (about 320 °C), to ensure that all liquid fuel is mixed with air.

E. Ignition System Unit

An electronic circuit is utilized to supply the electrodes with the necessary power to produce a forceful spark. The ignition system is made up of two parts: an electrical source (the battery) and an ignition coil. The coil is the part of the circuit that generates the high voltage (11000 V) from the 12 V battery. An electronic circuit is utilized to

supply the electrodes with the necessary power to produce a forceful spark. The ignition system is made up of two parts: an electrical source (the battery) and an ignition coil.

F. Fuel Injection and Control Unit

The amount of each fuel to be mixed is controlled by a control system that uses a programmed to control the opening, closing, and duration of the solenoid valves. To acquire precise fuel measurement, the valve's pulse width can be varied from 2 to 8 milliseconds, according to the valve's specifications. Tests have shown that a pulse width of 3 ms produces correct results for the appropriate fuel volumes.

G. Photograph Capturing Unit

The flame and flame propagation process are shown using the AOS - Q-PRI portable high-speed camera. It boasts a 3 Mega Pixel image resolution, 1.3 GB of internal memory, and a frame rate of 16,000 frames per second (FPS). The experiment was carried out with a camera with a resolution of (576*500 pixels) and a frame rate of 4229 frames per second (FPS). The overall duration of the recording is set to 1.2 seconds. When the triggers, ignition unit, and camera are all turned on, 10% of the time is set aside for pre-triggering to ensure that the entire procedure is recorded.

H. Measuring Instrumentations

Instruments such as temperature and pressure gauges are employed. A twelve-channel temperature recorder SD Card with real-time data logger is used to capture the thermocouple values (type Lutron BTM 4208SD). There are two type K thermocouples in use. The first thermocouple measures the temperature of the mixture inside the combustion chamber, which should be 320 degrees Celsius, and the second thermocouple measures the temperature of the air inside the hot air tank. A Bourdon pressure gauge is also used to measure the vacuum and starting pressure inside the combustion chamber (-1.0-3.0 bar). An isolating valve is a valve that closes during the combustion process to protect the pressure gauge from a rapid rise in combustion pressure. An electronic pressure gauge (0-100 bar) is connected to a data logger (DI-710-UH) installed in the upper flange to measure the combustion pressure.

3. Experimental Procedure

Initially, a vacuum pump is used to clear the combustion chamber of any air or residual gases from prior tests, after which it is purged with hot air and lastly vacuumed. The mixture is admitted from the pre-chamber (injectors chamber) to the main chamber via the connecting valve and is ready for ignition after the needed mixture of fuels and air is prepared in the pre-chamber according to blending ratio and equivalency ratio. After turning on the light and turning on the camera, the ignition system is turned on to generate the spark and start the combustion process. The stretched laminar flame speed is calculated using the recorded combustion films. For each test, the same protocol is followed.

4. Results and Discussions

Stretched laminar flame speed is the rate at which the flame front position (r) changes as a result of a photographic process. Experiments are carried out to measure the stretched laminar flame speed and equivalency ratios for several types of fuel mixtures at varied initial pressures (1,2 and 3 bar). To track the movement of the flame front, tracker software is utilized to extract data on the variation of flame radius over time. The instantaneous or extended flame speed is the slope of a line segment containing two neighboring radii versus time points (S_n), i.e.

$$S_n = \left. \frac{dr}{dt} \right|_{(j+1/2)} = \frac{r_{j+1} - r_j}{t_{j+1} - t_j} \quad (1)$$

The radius corresponds to this speed is taken to be the mean radius,

$$r_{(j+1/2)} = \frac{r_{j+1} + r_j}{2} \quad (2)$$

Different radii are obtained in different directions at the same time due to the uneven flame front shape. The flame front is hence non-spherical. As a result, the Tracker program calculates the radius in four directions and an average flame radius, which is then utilized in equation (3) to calculate the stretched flame speed.

$$S_n = \frac{dr}{dt} = \frac{(r_{i,j+n+1} - r_{i,j+n+2}) + (r_{i,j-n-1} - r_{i,j-n-2}) + (r_{i+n+1,j} - r_{i+n+2,j}) + (r_{i-n-1,j} - r_{i-n-2,j})}{t_{j+1} - t_j} \Big/ 4 \quad (3)$$

5. Parametric Study

A. Effect of Initial Pressure

Figures (3 and 4) present the stretched laminar flame speed at flame radius of 20 mm for stoichiometric mixture with different initial pressures and different hydrogen blends. Figure (3) shows that the stretched flame speed decreases with increasing initial pressure for pure gasoline (G) and gasoline-hydrogen mixture (G-H) for all hydrogen blending ratios due to increase in mixture density. However, the stretched flame speed increases with increase in hydrogen blending ratio for all tested initial pressure. This is due to the presence of hydrogen in the mixture which is characterized by its high flame speed.

Figure (4) shows the variation of stretched flame speed of triple fuel mixture, gasoline, hydrogen and ethanol (G-H-E) with different initial pressures, different blending ratios and stoichiometric mixture. The results show that the presence of the third fuel (ethanol) causes a reduction in the stretched flame speed slightly compared with the dual fuel (G-H). On the other hand, it causes an increase in the stretched flame speed compared with pure gasoline (G). Also, it can be observed that the increasing in the initial pressure causes a decrease in the stretched flame speed of all mixtures due to increasing the mixture density. Figure (5) depicts the fluctuation in stretched flame speed with initial pressure for constant hydrogen blending ratios and various (G-E) mixture blending ratios. The findings show that raising the ethanol blending ratio increases the extended flame speed. When the starting pressure is 1 bar, the maximum value is reached; however, when the initial pressure is increased, the maximum value drops.

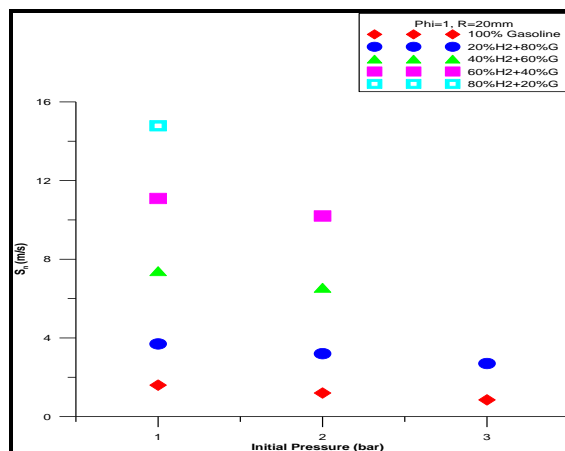
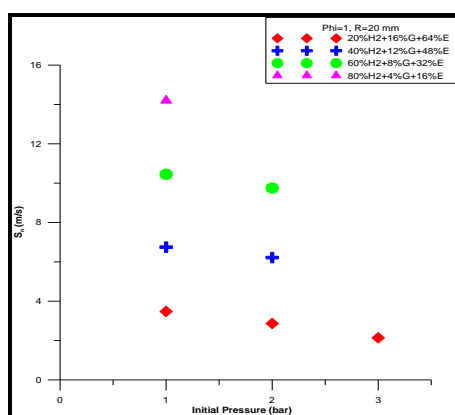
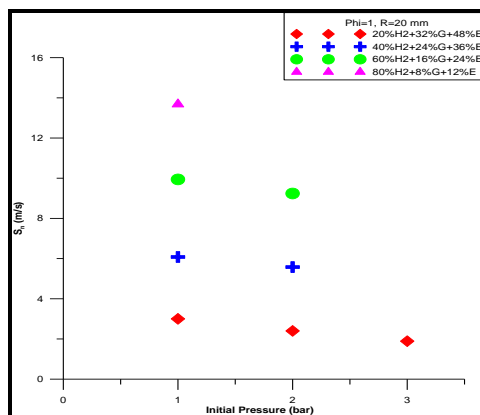


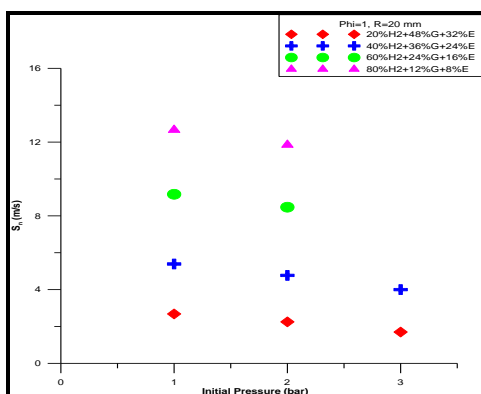
Fig. (3): Variation of S_n with Initial Pressures for Pure Gasoline (G) and for (G-H) mixture at Equivalence Ratio ($\phi = 1$) at Flame Radius of 20 mm.



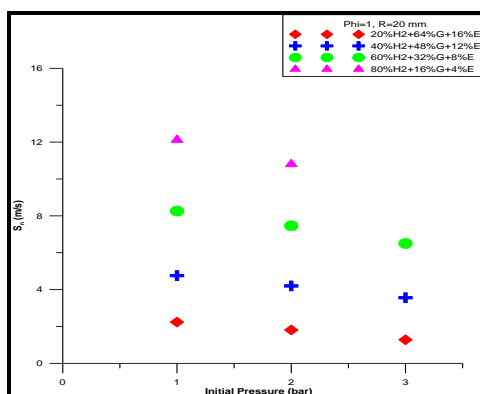
(a)



(b)



(c)



(d)

Fig. (4): Variation of S_n with Initial Pressures for Different Triple Fuel Mixtures (G-H-E) at Equivalence Ratio ($\phi = 1$) at Flame Radius of 20 mm

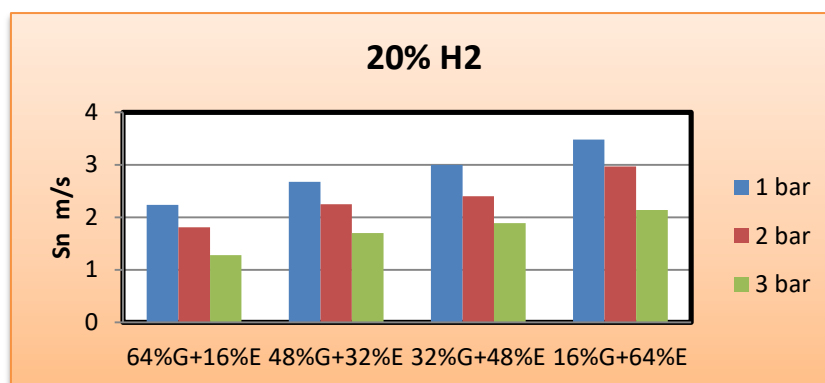


Fig. (5): Variation of S_n with Initial Pressure for 20% H with Different Blending Ratios of G-E

Figures (6 and 7) present the variations of un-stretched laminar flame speed with initial pressure for stoichiometric mixtures with different blending ratios. From these figures, it can be observed that the value of un-stretched laminar flame speed (S_u) decreases with increasing initial pressure due to increasing density of mixture which the same behavior of stretched flame speed with initial pressure. Figure (6) shows that the un-stretched flame speed increases with increasing hydrogen blending ratio due to higher flame speed of hydrogen and decreases with increasing initial pressure. The un-stretched flame speed values at atmospheric pressure and stoichiometric mixture for 100%G, 20%H-80%G, 40%H-60%G, 60%H-40%G and 80%H-20%G are 1.23 m/s, 3.67 m/s, 7.093 m/s, 10.79 m/s and 14.486 m/s respectively. These un-stretched flame speed decreases with initial pressure, for example, the un-stretched flame speeds of 20%H-80%G mixture at initial pressure 2 bar and 3 bar are 2.769 m/s and 2.26 m/s. For triple fuel mixes, Figure (7) depicts the fluctuation of un-stretched flame speed with beginning pressure (G-H-E). According to the findings, raising the hydrogen blending ratio for a mixture at the same pressure causes the un-stretched flame speed to increase due to the faster flame speed of pure hydrogen compared to pure ethanol fuel. By increasing the initial pressure this un-stretched flame speed of the mixture starts to decrease because of increasing the density of the mixture. Also, it can observe that the un-stretched flame speed of the (G-H-E) mixtures is lower than the G-H mixtures. Figure (8) shows the variation of the un-stretched flame speed with initial pressure for stoichiometric combustion at constant hydrogen blending ratio with different blending

ratios of G-E mixtures. The results show a significant effect of ethanol fuel where increasing blending ratio of ethanol fuel causes increasing un-stretched flame speed of the mixture for all tested pressure.

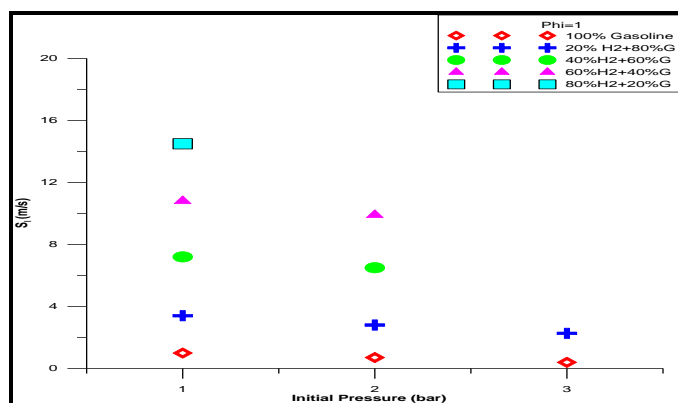


Fig. (6): Effect of Initial Pre. on Un-stretched Flame Speed for Pure Gasoline and H-G Stoi. Mix.

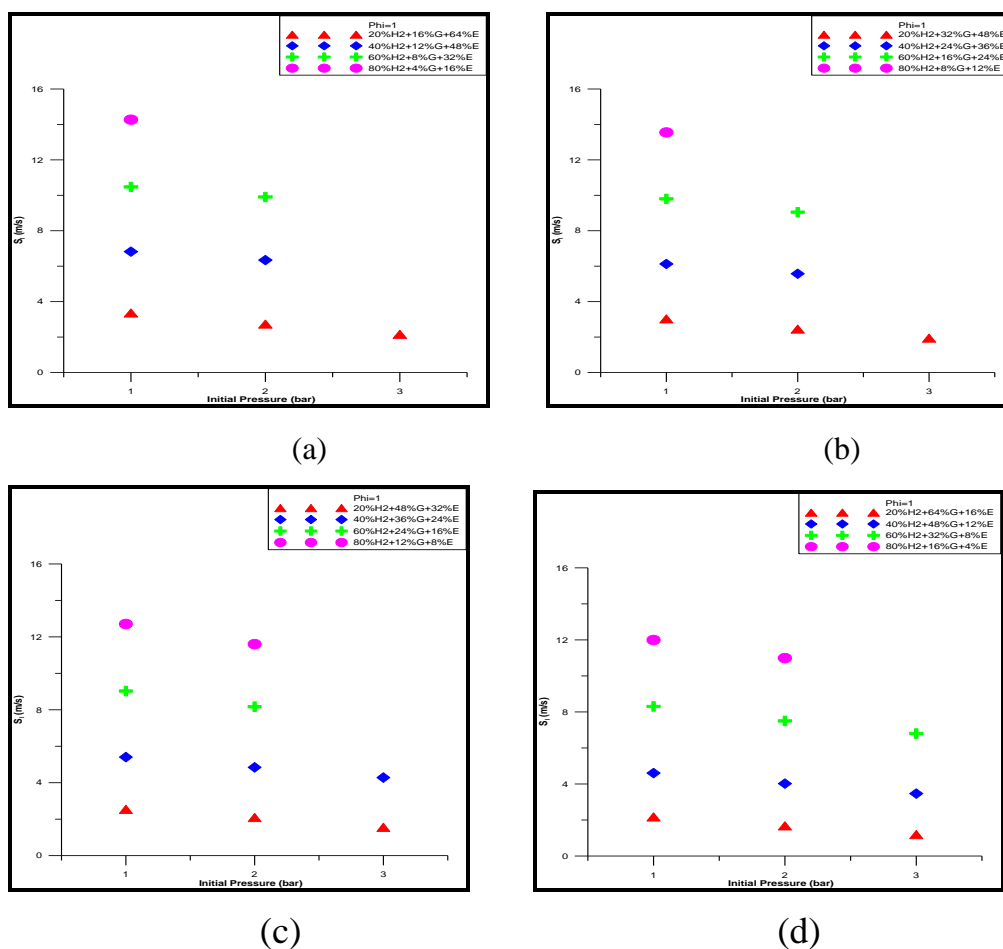


Fig. (7): Effect of Initial Pressure on Un-stretched Flame Speed for Different Blending Ratios of Triple Fuel Mixtures (H.G-E)

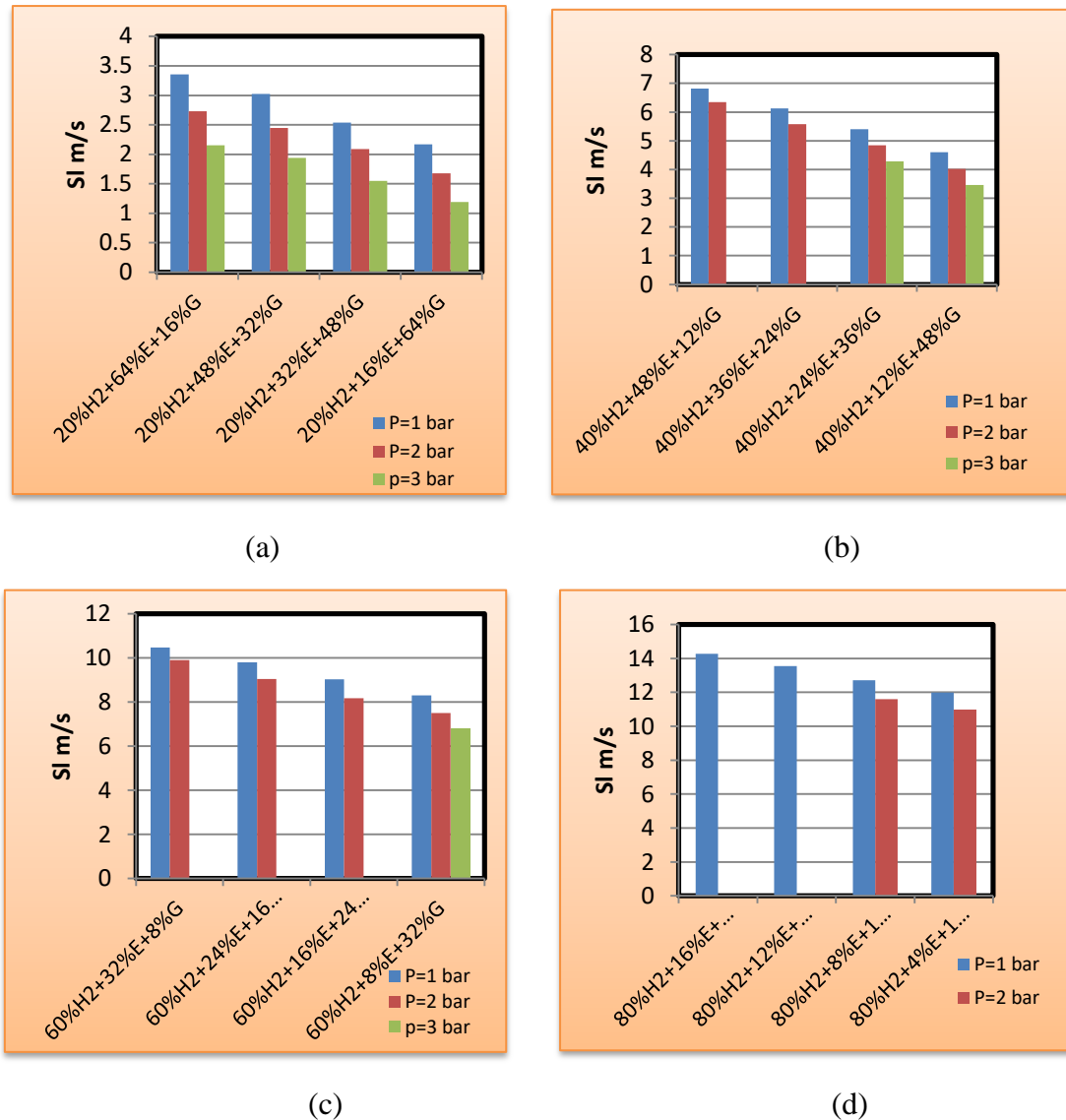


Fig. (8): Un-stretched Flame Speed with Different Initial Pressure of Stoichiometric Combustion for Different Blending Ratios of H- G- E Mixtures

B. Effect of Equivalence Ratio

Figures (9 and 10) show the effects of equivalency ratio on recorded flame speed for 100 percent G, G-H, and G-H-E mixes at atmospheric beginning pressure and a flame radius of 20 mm. These graphs illustrate that as the combination progresses from lean to stoichiometric, the flame speed increases, reaches a maximum value at (=1), and then drops as the mixture becomes richer. Figure (9), also, shows that the stretched flame speed increases with the increasing of hydrogen blending ratio in the dual fuel mixture for the same equivalence ratio due to high flame speed of hydrogen fuel. It is noticed

that the maximum flame speed is obtained at ($\Phi = 1$) for 100%G, and all other G-H blends. Figure (10) depicts the stretched flame speed of triple fuel (G-H-E) blends at 20 mm flame radius under atmospheric pressure. The results show that raising the hydrogen blending ratios with various (G-E) blending ratios increases the stretched flame speed, with the maximum value at the stoichiometric combination. This graph also illustrates that when the equivalency ratio grows, the measured stretched flame speed increases until it reaches its maximum value for a stoichiometric mixture. Any additional rise in equivalency ratios causes the stretched flame speed to decrease. All sorts of triple fuel mixtures follow the same pattern.

Figure (11) depicts the stretched flame speed at atmospheric pressure with a flame radius of 20 mm and various equivalency ratios for a constant hydrogen blending ratio with various (G-E) mixes. The results of this graph show that increasing the ethanol fuel blending ratio while keeping the hydrogen blending ratio constant increases the stretched flame speed of the combination, which peaks at stoichiometric combustion.

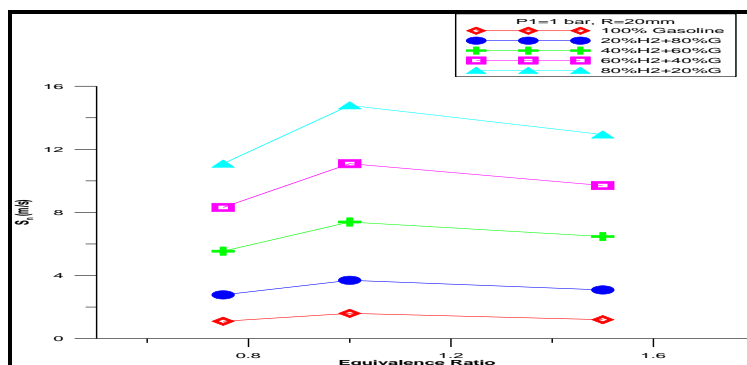
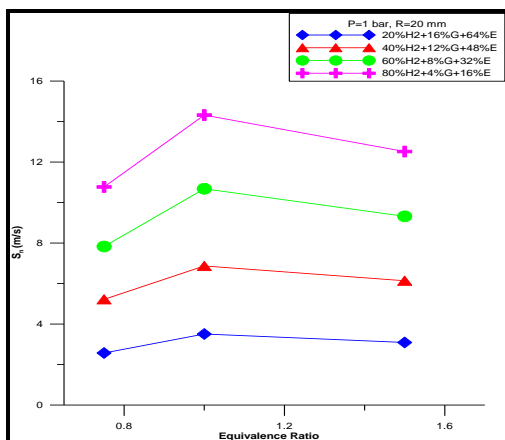
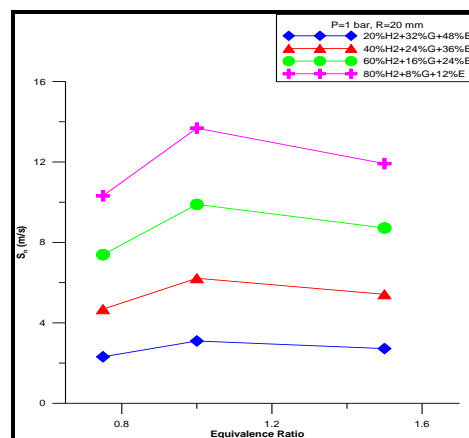


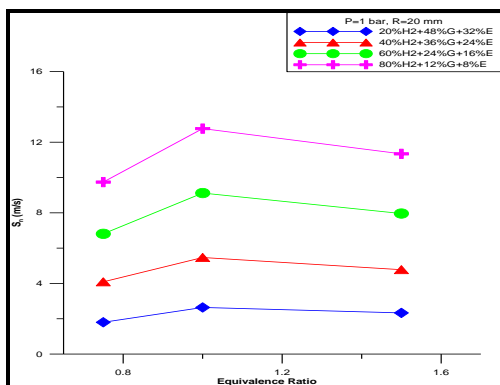
Fig. (9): Variation of S_n with Equivalence Ratios for 100%G and for G-H Blends at (20 mm) Radius and Atmosphere Pressure



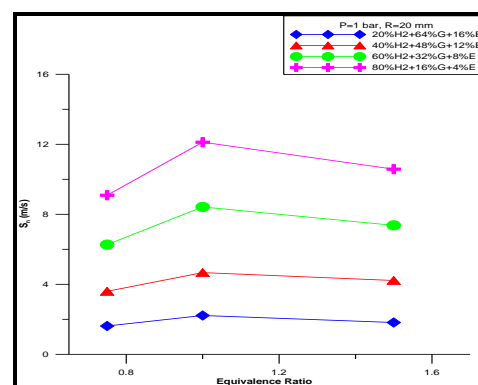
(a)



(b)

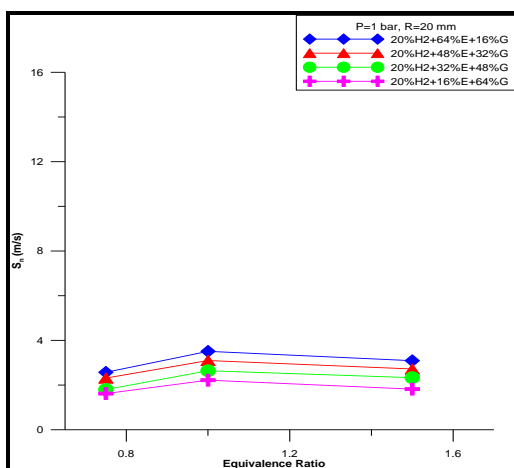


(c)

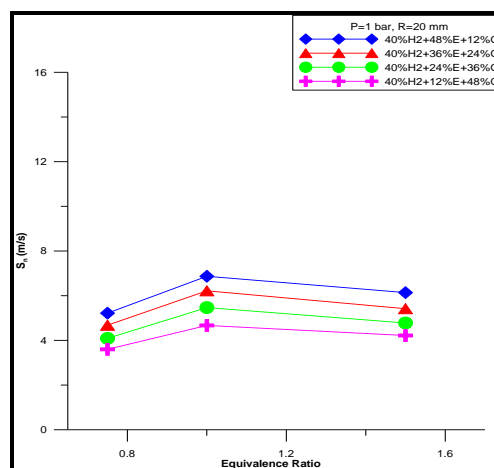


(d)

Fig. (10): Variation of S_n with Equivalence Ratios for Different G-H-E Mixtures at Atmospheric Pressure and at Flame Radius of 20 mm



(a)



(b)

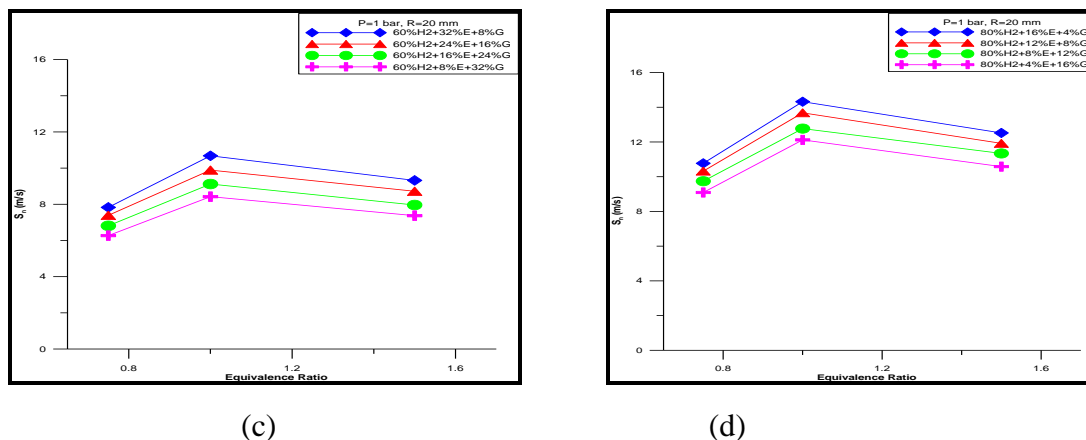


Fig. (11): Variation of S_n with Equivalence Ratios for Various G-E Mixtures at Flame Radius of 20 mm and Atmosphere Pressure for (a) 20% H, (b) 40% H, (c) 60% H and (d) 80% H

Figures (12 and 13) show the effect of equivalence ratio on the un-stretched flame propagation speed at atmospheric pressure for 100%G, other dual and triple fuel mixtures. The results of all tests show the un-stretched flame speed (S_1) approaches its maximum value as the mixture approaches the stoichiometric ratio. It is expected that the maximum value occurs on the slightly rich mixture which has the maximum adiabatic flame temperature. However, the un-stretched flame speed decreases as the mixture becomes richer for all types of mixtures. For pure 100 percent G and (G-H) mixes, Figure (12) displays the fluctuation of un-stretched flame speed with equivalency ratio. The results present that the maximum value occurs at stoichiometric mixture ($\phi=1$) due to the complete combustion and higher adiabatic flame temperature. Figure (13) depicts the variation in un-stretched flame speed with equivalency ratios for triple fuel combinations. (G-H-E). In the case of dual fuel blends, this picture displays the maximum un-stretched flame speed for stoichiometric combustion. Figure (14) shows how un-stretched flame speed varies with equivalence ratio when utilizing (G-E) mixes with a constant hydrogen blending ratio. This graph shows how increasing the ethanol fuel blending ratio increases the un-stretched flame speed. Because pure ethanol fuel has the fastest flame speed, it has a sufficient effect.

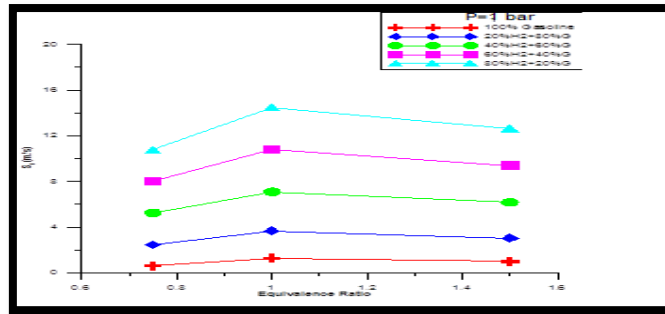
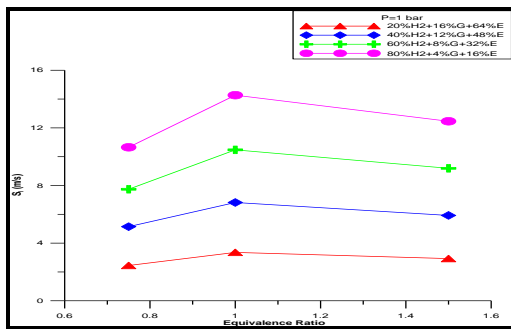
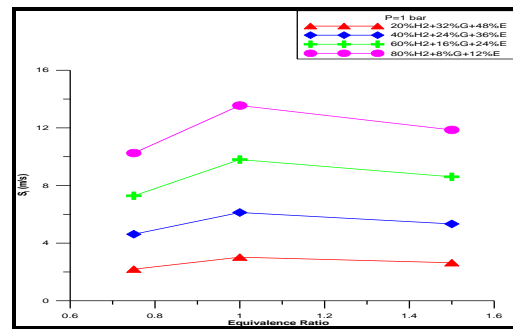


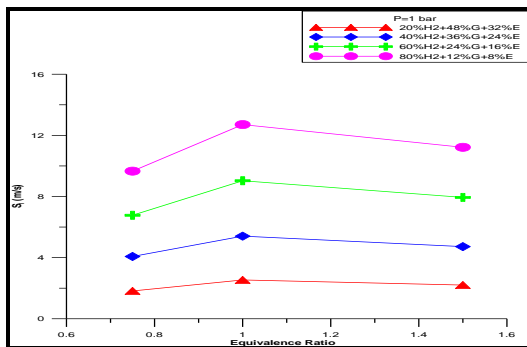
Fig. (12): Un-stretched Flame Speed Versus Equi. Ratios for 100%G and diff.G-H Mixtures



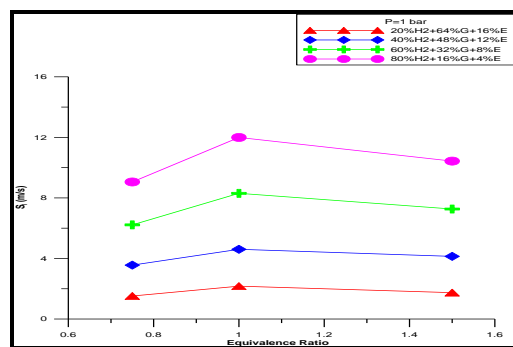
(a)



(b)



(c)



(d)

Fig. (13): Un-stretched Flame Speed Versus Equi. Ratios for Diff. Blending Ratios of (H-G-E)

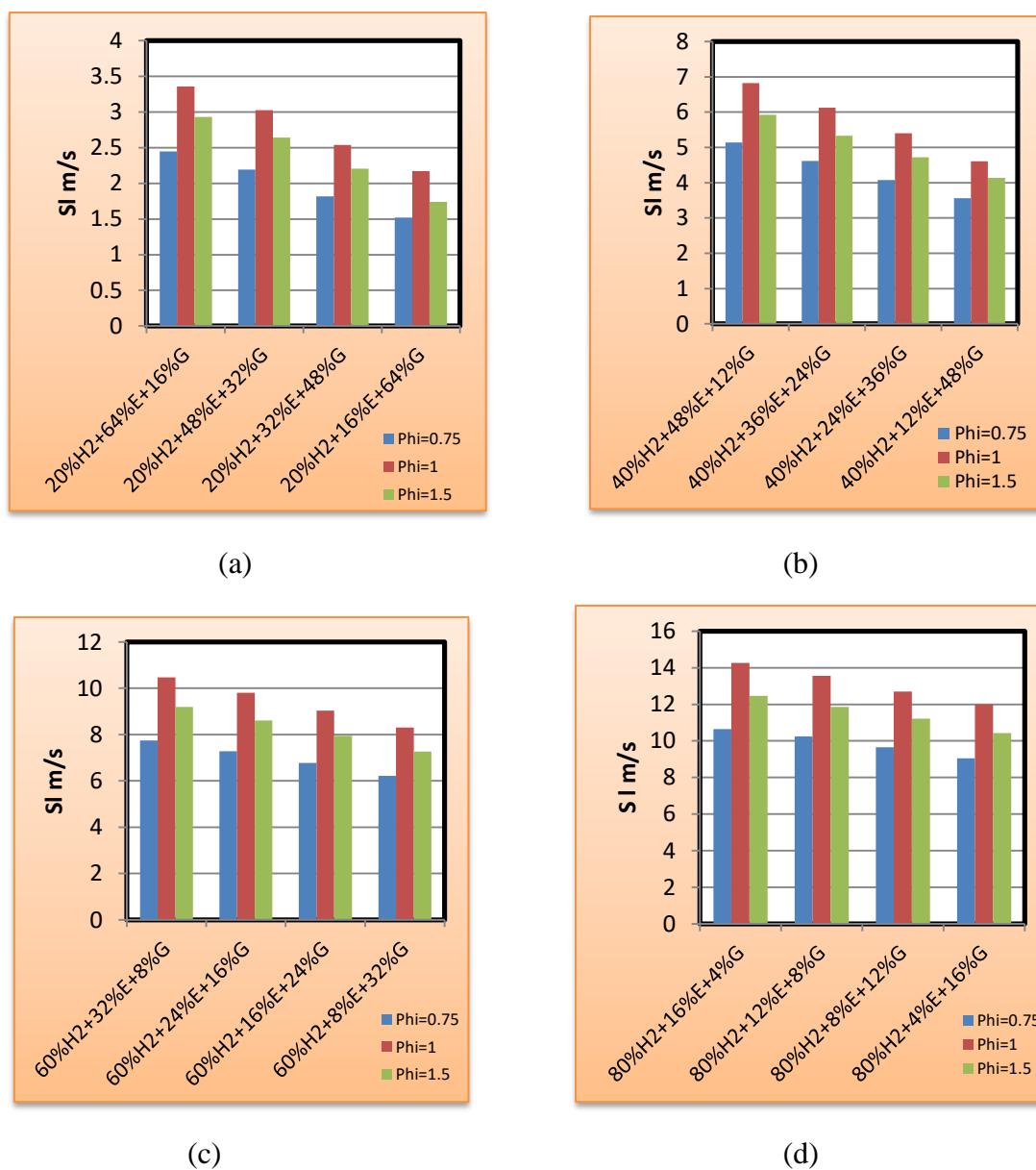


Fig. (14): Un-stretched Flam Speed Versus Equivalence Ratios for Different Blending Ratios of G-E Mixtures at Initial Pressure of 1 bar with different H ratios

6. Conclusions

With rising initial pressure, the speeds of both stretched and un-stretched flames decrease. The inclusion of hydrogen boosts the mixture's flame speeds, both stretched and un-stretched. The addition of ethanol at a constant hydrogen ratio enhances the mixture's flame speeds on both sides. For all blends, maximum flame speeds are found in a stoichiometric combination. Also, the conclusions can be illustrated as follows:

- 1- The un-stretched flame speed values at atmospheric pressure and stoichiometric mixture for 100%G, 20%H-80%G, 40%H-60%G, 60%H-40%G and 80%H-20%G are 1.23 m/s, 3.67 m/s, 7.093 m/s, 10.79 m/s and 14.486 m/s respectively.
- 2- Laminar burning velocity and flame speed increase as the hydrogen ratio of gasoline-hydrogen mixtures increases at pressure (1 bar) and stoichiometric combustion, with burning velocity increasing from 0.6 m/s (pure gasoline) to 2.99 m/s (80 percent hydrogen-20 percent gasoline) and flame speed increasing from 1.3 m/s (pure gasoline) to 14.79 m/s (80 percent hydrogen-20 percent gasoline).
- 3- The rising hydrogen ratio enhances laminar burning velocity and flame speed for triple fuel mixtures (gasoline-hydrogen-ethanol). Flame speeds for 20 percent H₂-64 percent G-16 percent E, 20 percent H₂-64 percent G-16 percent K, 40 percent H₂-48 percent G-12 percent E, and 40 percent H₂-48 percent G-12 percent K at pressure (1 bar) and stoichiometric combustion are 2.24 m/s, 1.99 m/s, 4.63 m/s, and 4.43 m/s, respectively, for 20 percent H₂-64 percent G-16 percent E, 20 percent H₂-64 percent G-16 percent K. At the same conditions, the burning velocity of the aforesaid triple fuel mixtures is 0.641 m/s, 0.623 m/s, 1.225 m/s, and 1.19 m/s, respectively.

References

1. Taylor, Simon Crispin "Burning velocity and the influence of flame stretch". Ph.D. thesis, Department of Fuel and Energy University of Leeds, UK, (1991).
2. 2-Y. Dong, C. M. Vagelopoulos, G. R. Spedding, and F. N. Egolfopoulos "Measurement of laminar flame speeds through digital particle image velocimetry: Mixtures of methane and ethane with hydrogen, oxygen, nitrogen, and helium," Proc. Combust. Inst., vol. 29, pp. 1419-1426, (2002).
3. Z. Zhao, J. P. Conley, A. Kazakov, and F. L. Dryer "Burning velocities of real gasoline fuel at 353 K and 500 K," SAE Int. , vol. 112, pp. 2624-2629, (2003).
4. K. J. Bosschaart and L. P. H. De Goey, "The laminar burning velocity of flames propagating in mixtures of hydrocarbons and air measured with the heat flux method," Combust. Flame, vol. 136, pp. 261-269, (2004).
5. Z. Zhao, "Experimental and numerical studies of burning velocities and kinetic modeling for practical and surrogate fuels". PhD: University of Princeton, (2005).
6. J. Natarajan, T. Lieuwen, and J. Seitzman, "Laminar flame speeds of H₂/CO mixtures: Effect of CO₂ dilution, preheat temperature, and pressure," Combust. Flame, vol. 151, pp. 104-119, (2007).
7. G. P. Smith, D. M. Golden, M. Frenklach, N. W. Moriarty, Z. B. Eiteneer, M. Goldenberg, T. Bowman, R. K. Hanson, S. Song, W. C. Gardiner, V. V. Lissianski, and Z. Qin, "GRI-Mech 3.0 Available from www.me.berkeley.edu/gri_mech/, (2016).
8. S. G. Davis, A. V. Joshi, H. Wang, and F. Egolfopoulos, "An optimized kinetic model of H₂/CO combustion", Proc. Combust. Inst., vol. 30, pp. 1283-1292, (2005).
9. Erjiang Hu, Zuohua Huang, Jianjun Zheng, Qianqian Li, Jiajia He, "Numerical study on laminar burning velocity and NO formation of premixed methane–hydrogen–air flames", International journal of Hydrogen Energy, vol. 34, pp. 6545- 6557, (2009).

10. T. Tahtouh, F. Halter, C. Mounaim-Rousselle, "Measurement of laminar burning speeds and Markstein length using a novel methodology", *Combustion and Flame*, vol. 156, pp. 1735-1743, 2009.
11. Ganeshan , *Internal Combustion Engine* ” third edition Published By the Tata McGraw-Hill Publishing Company Limited, 7 West Patel Nagar, New Delhi 110008. pp 372-375, (2010).
12. G. Broustail P. Seers F. Halter G. Moréac C. Mounaim-Rousselle, "Experimental determination of laminar burning velocity for butanol and ethanol iso-octane blends" *Journal of Fuel*, Vol. 90 Issue 1, (1–6), (2011) .
13. Hagos F., Aziz A., Sulaiman S. "Effect of air – fuel ratio on the combustion characteristics of syngas (H₂: CO) in direct injection spark ignition engine" *Energy Procedia* (2014) 61 2567-2571, (2014)
14. Ahmad Shakir and Haroun A. K. Shahad, “Experimental Study of the Effect of Hydrogen Blending on Burning Velocity of Different Fuels” M.Sc. Thesis, University of Babylon, (2016).
15. Oras Khudhayer and Haroun A. K. Shahad, “A Review of Laminar Burning Velocity and Flame Speed of Gases and Liquid Fuels”. *International Journal of Current Engineering and Technology* E-ISSN 2277 – 4106, P-ISSN 2347 – 5161 ©2017 INPRESSCO, Accepted 02 Feb 2017, Available online 12 Feb 2017, Vol.7, No.1 (Feb 2017).